



University of HUDDERSFIELD

University of Huddersfield Repository

Cryan, R.A., Unwin, Rodney T., Garrett, Ian, Sibley, Martin J.N. and Calvert, N.M.

Optical fibre digital pulse-position-modulation assuming a Gaussian received pulse shape

Original Citation

Cryan, R.A., Unwin, Rodney T., Garrett, Ian, Sibley, Martin J.N. and Calvert, N.M. (1990) Optical fibre digital pulse-position-modulation assuming a Gaussian received pulse shape. IEE Proceedings - Optoelectronics, 137 (2). pp. 89-96. ISSN 0267-3932

This version is available at <http://eprints.hud.ac.uk/id/eprint/2889/>

The University Repository is a digital collection of the research output of the University, available on Open Access. Copyright and Moral Rights for the items on this site are retained by the individual author and/or other copyright owners. Users may access full items free of charge; copies of full text items generally can be reproduced, displayed or performed and given to third parties in any format or medium for personal research or study, educational or not-for-profit purposes without prior permission or charge, provided:

- The authors, title and full bibliographic details is credited in any copy;
- A hyperlink and/or URL is included for the original metadata page; and
- The content is not changed in any way.

For more information, including our policy and submission procedure, please contact the Repository Team at: E.mailbox@hud.ac.uk.

<http://eprints.hud.ac.uk/>

Optical fibre digital pulse-position-modulation assuming a Gaussian received pulse shape

R.A. Cryan, BSc
R.T. Unwin, PhD, CEng, MIEE
I. Garrett, PhD, CEng, MIEE
M.J.N. Sibley, PhD
N.M. Calvert, PhD

Indexing terms: Pulse-code modulation, Optical fibres

Abstract: The abundance in bandwidth available in the best monomode fibres may be exchanged for improved receiver sensitivity by employing digital PPM. This paper presents a performance and optimisation analysis for a digital PPM coding scheme operating over a fibre channel employing a PIN-BJT receiver and assuming a Gaussian received pulse shape. We present original results for a 50 Mbit/s, 1.3 μm wavelength digital PPM system and conclude that, provided the fibre bandwidth is several times that of the data rate, digital PPM can outperform commercially available PIN-BJT binary PCM systems.

1 Introduction

Digital-pulse position modulation (PPM) is an attractive technique for trading the abundance of bandwidth available in monomode fibres operating near the wavelength of minimum chromatic dispersion, for improved receiver sensitivity. In the main, work presented in the literature considers digital PPM in the context of free-space communications [1–8]. Garrett [9–11] has analysed digital PPM systems operating over slightly dispersive optical channels using direct detection PIN-FET receivers and coherent receivers. Pires and da Rocha [12] have extended Garrett's performance and optimisation analysis to consider receivers employing avalanche photodiodes. By minimising bounds on the average error probability, they have developed a suboptimum PPM-APD receiver.

We present an analysis for digital PPM transmitted over optical-fibre channels employing PIN-BJT receivers and assuming a Gaussian-received pulse shape. We adopt a variational calculus approach to derive an optimal filter for estimating the arrival time of the pulse. The optimal filter is shown to be a matched filter in cascade with a

proportional-derivative-delay network. Thus, the employment of a PIN-BJT pre-amplifier reduces the complexity of the receiver design in comparison to the PIN-FET preamplifier [11], in that the noise whitening filter may be dispensed with.

Computer-predicted results are presented for a 50 Mbit/s, 1.3 μm digital PPM system assuming a Gaussian-received pulse shape. We conclude that the digital PPM system should achieve an improvement in sensitivity of typically 7.5 dB, over commercially available binary PCM transimpedance PIN-BJT receivers.

2 System models

The model for digital PPM is illustrated in Fig. 1. M bits (termed the coding level) of binary PCM are converted to

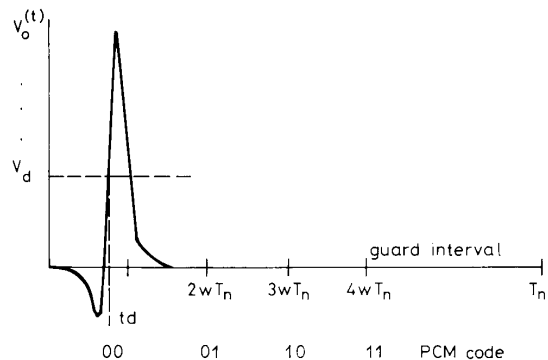


Fig. 1 Digital PPM model

digital PPM in a time frame length T_m and transmitted by sending a single pulse in one of $n = 2^M$ time slots, each of width wT_n . The n time slots are contained in the fraction $m < 1$ of the frame, where $m = nw$ is the modulation depth. A guard interval $(1 - m)T_n$ is included at the end of each frame, for timing extraction purposes and to prevent interframe interference due to dispersion.

The receiver is synchronised to the transmitter by a clock which may be derived from the digital PPM pulse stream. At an instant t_d relative to this clock signal, the receiver output voltage $v_o(t)$ crosses a threshold level v_d with positive slope. The received symbol is determined by whichever of the n slots contain t_d .

The receiver model for a direct-detection transimpedance PIN-BJT preamplifier is illustrated in Fig. 2.

Paper 7187J (E13), received 3rd July 1989

Dr. Sibley, Dr. Unwin and Mr. Cryan are with the Department of Electrical and Electronic Engineering, The Polytechnic, Huddersfield, W. Yorkshire HD1 3DH, United Kingdom

Dr. Garrett is with BTRL, Martlesham Heath, Ipswich IP5 7RE, United Kingdom

Dr. Calvert is with TriCom Communications Ltd, Oxford Road, Stokenchurch, High Wycombe, Buckinghamshire HP14 3SX, United Kingdom

The preamplifier input impedance is the parallel combination of a capacitance C_a and a resistance R_a . We model the detector as an ideal photodiode in parallel with a capacitance C_d . The resistance R_b represents the transistor DC bias and the detector DC return resistance.

occurs at time t_p , $\langle n_o(t)^2 \rangle =$ mean-square receiver output noise.

3.1.2 Wrong slot errors: These occur when noise on the leading edge of the pulse produces a threshold crossing in

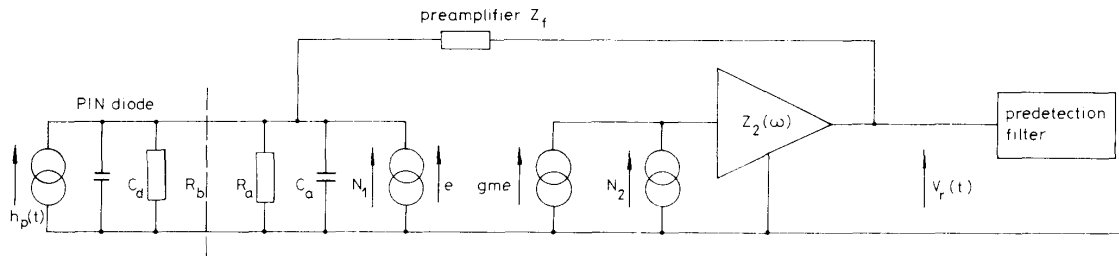


Fig. 2 Receiver model

N_1 and N_2 are the current noise generators representing the input and output noise sources associated with the first stage of the preamplifier. The receiver model is identical to that used for binary PCM, except that the predetection filter is replaced by the optimal filter derived in Section 3.3.

3 Analysis

3.1 Error sources

Fig. 3 illustrates the three sources of error in estimating the arrival time of the pulse.

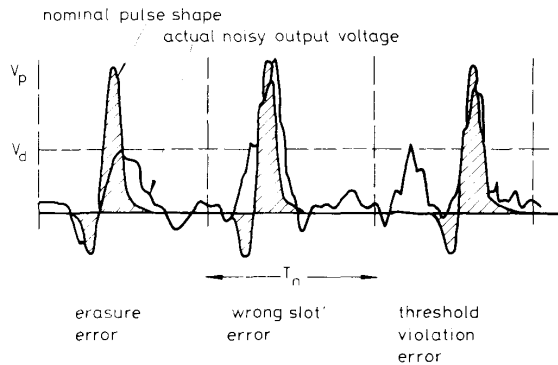


Fig. 3 Error sources

3.1.1 Erasures: An erasure error occurs whenever noise destroys the pulse, thus preventing detection. The probability of an erasure error P_r , assuming the receiver output noise voltage is a Gaussian random-variable, is

$$P_r = 0.5 \operatorname{erfc} \left(\frac{Q_r}{\sqrt{2}} \right) \quad (1)$$

where

$$Q_r^2 = \frac{(v_p - v_d)^2}{\langle n_o(t)^2 \rangle} \quad (2)$$

and $v_d = v_o(t_d) =$ receiver output at the threshold crossing time, $v_p = v_o(t_p) =$ peak receiver output voltage which

the time slot immediately preceding or following that containing the pulse. The probability of a wrong slot error P_s is given by

$$P_s = \operatorname{erfc} \left(\frac{Q_s}{\sqrt{2}} \right) \quad (3)$$

where

$$Q_s^2 = \left(\frac{mT_n}{2n} \right)^2 \frac{1}{\langle n_o(t)^2 \rangle} \left(\frac{dv_o}{dt} \Big|_{t_d} \right)^2 \quad (4)$$

3.1.3 False-alarm errors: In the interval between the start of the frame and the arrival of the signal pulse, the receiver output voltage may cross the threshold, owing to noise with probability

$$P_t = \operatorname{erfc} \left(\frac{Q_t}{\sqrt{2}} \right) \quad (5)$$

where

$$Q_t^2 = \frac{v_d^2}{\langle n_o(t)^2 \rangle} \quad (6)$$

The numbers of uncorrelated samples per time slot can be estimated in terms of the time τ_r , at which the autocorrelation function of the receiver filter has become small, as $(mT_n/n\tau_r)$. The probability per time slot of false alarm error is then approximated by [13]

$$P_f = \left(\frac{mT_n}{n\tau_r} \right) P_t \quad (7)$$

when $P_f \ll 1$.

3.2 Performance criterion

A digital PPM transmitter emits a set of symbols $x_i \in [x_r]_{r=1}^n$ which consist of the n equiprobable pulse positions, and the receiver receives a set $y_j \in [y_r]_{r=1}^{n+1}$ consisting of the n pulse positions plus erasures. We specify, as our performance criterion, that the equivocation rate of the digital PPM system should be the same as in a binary PCM system, with the same source entropy rate and with an error probability of 10^{-9} . The equivocation rate of the

digital PPM system can be written as

$$H(X|Y) = - \sum_{i=1}^n \sum_{j=1}^{n+1} P(x_i)P(y_j|x_i) \log [P(y_j|x_i)] \quad (8)$$

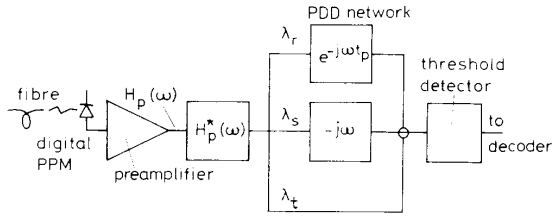


Fig. 4 The optimal filter

and so we need to evaluate $P(Y|X)$. As we are assuming a threshold-crossing detector, false-alarm errors can only occur in the time slots preceding the pulse. If the pulse is in slot k , and P_f is small, the probability of a threshold violation is approximately $(k-1)P_f$. Wrong slot errors can only occur in the time slots either side of that containing the pulse, whereas erasure errors can only occur in the slot containing the pulse. Hence, for a pulse in slot k :

$$\begin{aligned} P(0|k) &= P_r && \text{(an erasure)} \\ P(1|k), \dots, P(k-2|k) &= P_f && \text{(false alarm)} \\ P(k-1|k) &= P_f + \frac{P_s}{2} \\ P(k|k) &= 1 - P_s - P_r - (1-k)P_f && \text{(correct detection)} \\ P(k+1|k) &= \frac{P_s}{2} \\ P(k+2|k), \dots, P(n|k) &= 0 \end{aligned}$$

By enumeration for a given k , and averaging over all k , we find

$$\begin{aligned} H(X|Y) &= -P_r \log_2(P_r) - \left(P_f + \frac{P_s}{2}\right) \\ &\quad \times \log_2\left(P_f + \frac{P_s}{2}\right) - \left(\frac{P_s}{2}\right) \log_2\left(\frac{P_s}{2}\right) \\ &\quad + P_s + P_r - \left(\frac{P_f}{2}\right) \\ &\quad \times [(n-3) \log_2(P_f) - (n-1)] \quad (9) \end{aligned}$$

The mean PCM equivocation rate per frame of $\log_2(n)$ bits is given by

$$H_{PCM}(X|Y) = [(1 - P_e) \log_2(1 - P_e) + P_e \log_2(P_e)] \log_2(n) \quad (10)$$

Defining the partial equivocation due to erasure errors as

$$H_r(X|Y) = -P_r \log_2(P_r) + P_r \quad (11)$$

the partial equivocation due to wrong slot errors as

$$H_s(X|Y) = P_s - \left(\frac{P_s}{2}\right) \left[\log_2\left(\frac{P_s}{2}\right) + \log_2\left(P_f + \frac{P_s}{2}\right) \right] \quad (12)$$

the partial equivocation due to false alarm errors as

$$\begin{aligned} H_f(X|Y) &= -P_f \log_2\left(P_f + \frac{P_s}{2}\right) - \left(\frac{P_f}{2}\right) \\ &\quad \times [(n-3) \log_2(P_f) - (n-1)] \quad (13) \end{aligned}$$

which are independent under the conditions $P_f \ll P_s$ or $P_f \gg P_s$, which is generally true except for a small range of fibre bandwidths. Thus, the performance criterion becomes

$$H_r(X|Y) + H_s(X|Y) + H_f(X|Y) - H_{PCM}(X|Y) = 0 \quad (14)$$

3.3 The optimal filter

We represent the predetection filter as a linear filter with transfer function $G(\omega)$ and impulse response $g(t)$. For a transimpedance PIN-BJT preamplifier, the output noise spectrum is approximately white with power spectral density S_0 [14]. Thus, the mean-square noise at the filter output is given by

$$\langle n_0(t)^2 \rangle = S_0 \int_{-\infty}^{\infty} g^2(t) dt \quad (15)$$

If we denote the preamplifier output voltage as $v_{pa}(t)$, then the filter output voltage becomes

$$\langle v_0(t) \rangle = g(t) * v_{pa}(t) = \int_{-\infty}^{\infty} g(\tau) v_{pa}(t - \tau) d\tau \quad (16)$$

The filter output voltage at the threshold crossing instant (which can be taken as $t = 0$ without loss of generality), its slope and the peak output voltage ($t = t_p$) are

$$v_d = \langle v_0(0) \rangle = \int_{-\infty}^{\infty} g(\tau) v_{pa}(-\tau) d\tau \quad (17)$$

$$v'_d = \left. \frac{d\langle v_0(t) \rangle}{dt} \right|_{t=0} = \int_{-\infty}^{\infty} g(\tau) v'_{pa}(-\tau) d\tau \quad (18)$$

$$v_p = \langle v_0(t_p) \rangle = \int_{-\infty}^{\infty} g(\tau) v_{pa}(t_p - \tau) d\tau \quad (19)$$

The optimal function $g(t)$ minimises $\langle n_0(t)^2 \rangle$ subject to constrained v_d , v'_d , v_p and can be derived by variational calculus. The Lagrangian is

$$\begin{aligned} L &= S_0 \int_{-\infty}^{\infty} g^2(\tau) d\tau + \lambda_f \int_{-\infty}^{\infty} g(\tau) v_{pa}(-\tau) d\tau \\ &\quad + \lambda_s \int_{-\infty}^{\infty} g(\tau) v'_{pa}(-\tau) d\tau \\ &\quad + \lambda_r \int_{-\infty}^{\infty} g(\tau) v_{pa}(t_p - \tau) d\tau \quad (20) \end{aligned}$$

The condition for a stationary point in L yields a filter impulse response given by

$$g(t) = \frac{1}{S_0} [\lambda_f v_{pa}(-t) - \lambda_s v'_{pa}(-t) + \lambda_r v_{pa}(t_p - t)] \quad (21)$$

with Fourier transform

$$G(\omega) = \frac{V_{pa}^*(\omega)}{S_0} [\lambda_f - j\omega\lambda_s + \lambda_r e^{-j\omega t_p}] \quad (22)$$

in which the signs have been chosen to give the threshold crossing on the positive-going edge of the pulse. The Lagrangian multipliers λ_r , λ_s and λ_t are factors which are

to be determined in terms of the system parameters. $G(\omega)$ contains an arbitrary scalar factor, thus it is possible to write

$$\lambda_f + \lambda_s + \lambda_r = 1 \quad (23)$$

Hence, there are two independent multipliers to be determined. The optimal filter consists of a matched filter in cascade with a proportional-derivative-delay network and is illustrated in Fig. 4. Note that, unlike direct detection employing PIN-FET preamplifiers [11], a noise whitening filter is not required, and so the receiver design is simplified.

4 Calculated results for Gaussian received pulses

For a received pulse energy b and pulse shape $h_p(t)$ such that

$$\int_{-\infty}^{\infty} h_p(t) dt = 1$$

the preamplifier output voltage is

$$\begin{aligned} \langle v_{pa}(t) \rangle &= bRZ_t(t) * h_p(t) \\ &= \frac{bR}{2\pi} \int_{-\infty}^{\infty} Z_t(\omega) H_p(\omega) e^{j\omega t} d\omega \end{aligned} \quad (24)$$

where R is the photodiode responsivity. Assuming the preamplifier has a single-pole frequency response, then

$$Z_t(\omega) = \frac{Z_t}{1 + j\left(\frac{\omega}{\omega_c}\right)} \quad (25)$$

where Z_t is the low-frequency transimpedance and ω_c is the preamplifier -3 dB bandwidth. The output of the optimal filter may now be expressed as

$$\begin{aligned} \langle v_o(t) \rangle &= bRZ_t(t) * h_p(t) * g(t) \\ &= \frac{bRZ_t}{2\pi S_0} \int_{-\infty}^{\infty} \frac{|H_p(\omega)|^2}{1 + \left(\frac{\omega}{\omega_c}\right)^2} \\ &\quad \times [\lambda_f - j\omega\lambda_s + \lambda_r e^{-j\omega t_p}] e^{j\omega t} d\omega \end{aligned} \quad (26)$$

Let us define a group of bandwidth-like integrals:

$$J_k = I_k(0) \quad \text{and} \quad K_k = I_k(t_p) \quad (27)$$

given by

$$I_k(t) = \frac{(j\omega T_n)^k}{2\pi S_0} \int_{-\infty}^{\infty} \frac{|H_p(\omega)|^2}{1 + \left(\frac{\omega}{\omega_c}\right)^2} e^{j\omega t} d\omega \quad (28)$$

The normalised Gaussian received pulse shape is defined as

$$h_p(t) = \frac{1}{\sqrt{(2\pi)\alpha}} \exp\left(-\frac{t^2}{2\alpha^2}\right) \quad (29)$$

$$H_p(\omega) = \exp\left(-\frac{(\alpha\omega)^2}{2}\right) \quad (30)$$

Consequently, the J and K integrals become

$$\begin{aligned} I_0(t) &= \frac{\omega_c}{4S_0} e^{(\alpha\omega_c)^2} \left[2 \cosh(\omega_c t) - e^{-\omega_c t} \right. \\ &\quad \left. \times \operatorname{erf}\left(\alpha\omega_c - \frac{t}{2\alpha}\right) - e^{\omega_c t} \operatorname{erf}\left(\alpha\omega_c + \frac{t}{2\alpha}\right) \right] \end{aligned} \quad (31)$$

$$\begin{aligned} I_1(t) &= \frac{T_n \omega_c^2}{4S_0} e^{(\alpha\omega_c)^2} \left[2 \sinh(\omega_c t) + e^{-\omega_c t} \right. \\ &\quad \left. \times \operatorname{erf}\left(\alpha\omega_c - \frac{t}{2\alpha}\right) - e^{\omega_c t} \operatorname{erf}\left(\alpha\omega_c + \frac{t}{2\alpha}\right) \right] \end{aligned} \quad (32)$$

$$\begin{aligned} I_2(t) &= \frac{T_n^2 \omega_c^3}{4S_0} e^{(\alpha\omega_c)^2} \left[e^{-\omega_c t} \left(\operatorname{erfc}\left(\alpha\omega_c - \frac{t}{2\alpha}\right) \right. \right. \\ &\quad \left. \left. - \frac{1}{\alpha\omega_c \sqrt{\pi}} e^{-(\alpha\omega_c - t/(2\alpha))^2} \right) + e^{\omega_c t} \left(\operatorname{erfc}\left(\alpha\omega_c + \frac{t}{2\alpha}\right) \right. \right. \\ &\quad \left. \left. - \frac{1}{\alpha\omega_c \sqrt{\pi}} e^{-(\alpha\omega_c + t/(2\alpha))^2} \right) \right] \end{aligned} \quad (33)$$

Recasting eqns. 15 and 17–19 in terms of these integrals gives:

$$v_d = bRZ_t[\lambda_r K_0 - \lambda_s J_1 + \lambda_f J_0] \quad (34)$$

$$v_p = bRZ_t[\lambda_r J_0 - \lambda_s K_1 + \lambda_f K_0] \quad (35)$$

$$v'_d = bRZ_t[\lambda_r K_1 - \lambda_s J_2 + \lambda_f J_1] \quad (36)$$

$$\begin{aligned} \langle n_0(t)^2 \rangle &= -\lambda_s^2 J_2 + (\lambda_r^2 + \lambda_f^2) J_0 \\ &\quad + 2\lambda_r \lambda_s K_0 + 2\lambda_r \lambda_s K_1 \end{aligned} \quad (37)$$

The error function arguments, eqns. 2, 4 and 6, may now be expressed as

$$Q_s^2 = (bRZ_t)^2 \left[\frac{mT_n}{2n} \right]^2 \frac{[\lambda_r K_1 - \lambda_s J_2]^2}{\langle n_0(t)^2 \rangle} \quad (38)$$

$$Q_r^2 = (bRZ_t)^2 \frac{[\lambda_r(J_0 - K_0) + \lambda_s K_1 + \lambda_f(K_0 - J_0)]^2}{\langle n_0(t)^2 \rangle} \quad (39)$$

$$Q_i^2 = (bRZ_t)^2 \frac{[\lambda_r K_0 + \lambda_f J_0]^2}{\langle n_0(t)^2 \rangle} \quad (40)$$

From which the error probabilities P_s , P_r and P_i may be determined.

It is more revealing to calculate the receiver sensitivity in terms of the system variables $[v, t_p]$ ($v = v_d/v_p$) which are related to the Lagrangian multipliers through the following equations:

$$v = \frac{v_d}{v_p} = \frac{\lambda_r K_0 + \lambda_f J_0}{\lambda_r J_0 + \lambda_s K_1 + \lambda_r K_0} \quad (41)$$

and

$$v'_p = \left(\frac{d\langle v_0(t) \rangle}{dt} \right)_{t=t_p} = -\lambda_s K_2 - \lambda_f K_1 = 0 \quad (42)$$

Eqns. 23, 41 and 42 may be solved simultaneously and the solution written as

$$\begin{bmatrix} \lambda_r \\ \lambda_s \\ \lambda_f \end{bmatrix} = \begin{bmatrix} 1 & 1 & 1 \\ 0 & -K_2 & -K_1 \\ K_0 - vJ_0 & -vK_1 & J_0 - vK_0 \end{bmatrix}^{-1} \begin{bmatrix} 1 \\ 0 \\ 0 \end{bmatrix}$$

In order to determine the probability of false-alarm errors (eqn. 7), we require τ_r , the time at which the autocorrelation function of the receiver filter has become small. The autocorrelation function for the Gaussian received pulse is

$$R_{xx}(\tau) \propto \alpha^3 \frac{\sqrt{\pi}}{2} \left(1 - \frac{\tau^2}{2\alpha^2} \right) \exp\left(-\frac{\tau^2}{2\alpha^2}\right) \quad (43)$$

This crosses zero at $\tau = \sqrt{2}\alpha$ and then approaches zero asymptotically from below. We will take $\tau_r = \alpha$ as a conservative estimate in calculating P_f .

The receiver sensitivity can now be optimised in terms of the system variables $[v, t_p]$. For a given pulse shape and assumed values of $[v, t_p]$ the J and K integrals are calculated, from which the Lagrangian multipliers may be determined and, hence, the error probabilities in terms of the pulse energy b . An inner iterative loop determines the value of b that satisfies the performance criterion given by eqn. 14. The system parameters $[v, t_p]$ are optimised by standard numerical techniques.

Calculations of receiver sensitivity were performed for a system at $1.3 \mu\text{m}$ wavelength, using the following practical receiver parameters for a CC-CE PIN-BJT pre-amplifier [15]: receiver bandwidth of 480 MHz, noise level of $3.2 \text{ pA}/\sqrt{\text{Hz}}$ and transimpedance $R_f = 5 \text{ k}\Omega$.

Fig. 5 illustrates the pulse shape at the matched filter output, for various fibre bandwidths which are normal-

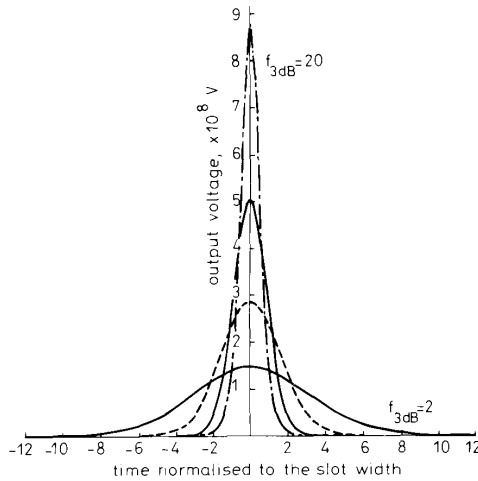


Fig. 5 Matched filter output voltage at 50 Mbit/s with $n = 128$ and $m = 0.8$

- normalised fibre bandwidth = 2.0
- - - normalised fibre bandwidth = 4.0
- · · normalised fibre bandwidth = 8.0
- · - normalised fibre bandwidth = 20.0

ised to the PCM data rate. In the low-bandwidth region, the pulse is dispersed and so the rise time is large in comparison to the slot width. To sharpen the rise time and minimise wrong slot errors, the PDD network weightings have the values shown in Fig. 6. A comparatively large derivative component λ_s , small erasure component λ_r , and large proportional component λ_f , employed in the low-fibre-bandwidth case results in the pulse shape of Fig. 7. The effect of the pulse shaping has indeed improved the pulse rise time, the negative precursor arising owing to the subtraction of the derivative contribution. Fig. 8 shows the partial equivocations as a function of fibre bandwidth. It can be seen that even with the corrective action of the PDD network, the partial equivocation attributed to wrong slot errors is dominant. The pulse rise time could be further sharpened by increasing the derivative contributions of the PDD network. However, an increased derivative contribution reduces the detection threshold level (the value at $t = 0$ in Fig. 7) and increases the noise level. Therefore, in the low-bandwidth region, the pulse energy is minimised by a tradeoff between the pulse rise time and the noise band-

width. With reference to Fig. 8, it can be seen that the performance criterion of eqn. 14 is maintained by ensuring $H_f(X|Y)$ and $H_r(X|Y)$ are small, to allow for the

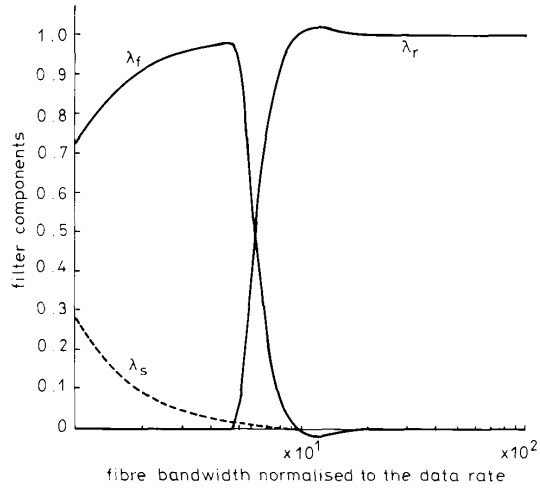


Fig. 6 Filter components as a function of fibre bandwidth at 50.0 Mbit/s with $n = 128$ and $m = 0.8$

- delayed filter component λ_r
- - - derivative filter component λ_s
- · - proportional filter component λ_f

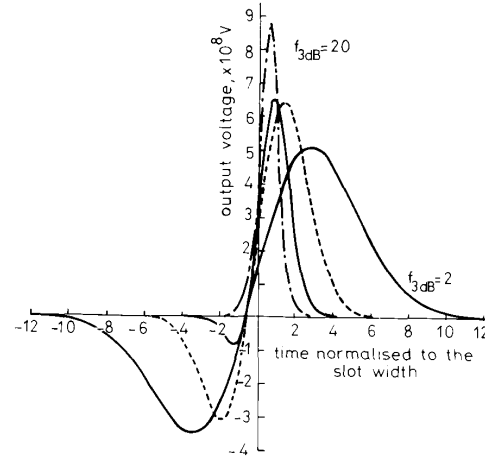


Fig. 7 Proportional-derivative-delay network output voltage at 50.0 Mbit/s with $n = 128$ and $m = 0.8$

- normalised fibre bandwidth = 2.0
- - - normalised fibre bandwidth = 4.0
- · · normalised fibre bandwidth = 8.0
- · - normalised fibre bandwidth = 20.0

dominant $H_s(X|Y)$. This is achieved by having a large pulse energy, which results in the threshold level being sufficiently high above the noise to minimise $H_f(X|Y)$ and $H_r(X|Y)$. Accordingly, as shown in Fig. 9, the receiver sensitivity ($P_e = 10^{-9}$) is relatively poor for low fibre bandwidths.

As the fibre bandwidth is increased, the output of the matched filter (Fig. 5) becomes less dispersed. Wrong slot errors become less significant, and so the requirement for the derivative contribution (Fig. 6) decreases. Fig. 8 shows that the partial equivocation attributed to wrong slot errors, $H_s(X|Y)$, begins to decrease and is compensated for by increasing $H_f(X|Y)$ and $H_r(X|Y)$ to maintain eqn. 14. This increase in $H_f(X|Y)$ and $H_r(X|Y)$ is

accomplished by a suitable selection of the Lagrangian multipliers and by reducing the pulse energy. For this reason, we see the improvement in receiver sensitivity as

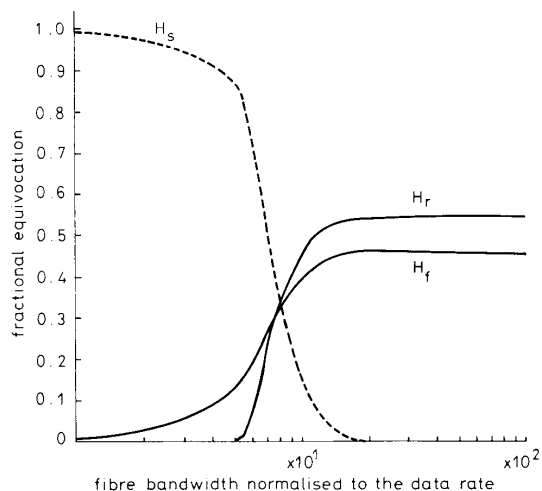


Fig. 8 Fractional equivocations plotted as a function of fibre bandwidth at 50.0 Mbit/s with $n = 128$ and $m = 0.8$

— $H_r(X|Y)$
 - - - $H_s(X|Y)$
 — $H_f(X|Y)$

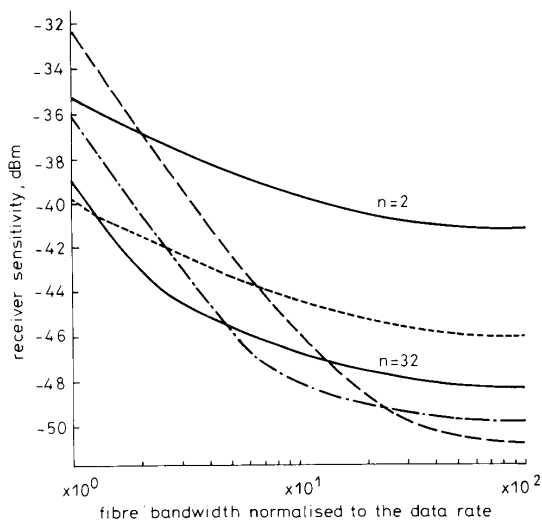


Fig. 9 Receiver sensitivity as a function of fibre bandwidth at 50.0 Mbit/s with $m = 0.8$

— $n = 2$
 - - - $n = 8$
 — $n = 32$
 - - - $n = 128$
 - - - $n = 512$

fibre bandwidth is increased, displayed in Fig. 9. Fig. 6 shows that, in this region, a transition takes place between λ_f and λ_r . The net effect of this is to increase the threshold level such that $v > 0.5$ to counter the relatively large $H_f(X|Y)$ which is n -dependant ($n = 128$). Both Figs. 6 and 8 depict the regions of different estimation strategy. In the low-bandwidth region, the pulse energy is minimised by a balance between false-alarm errors and wrong-slot errors. As fibre bandwidth increases, a transition takes place and the pulse energy is then minimised

by a trade-off between false-alarm errors and erasure errors.

The improvement in receiver sensitivity continues until the fibre bandwidth approaches the bandwidth of the PIN-BJT preamplifier. At this point, any further increase in fibre bandwidth leads to very little improvement in receiver sensitivity, because the preamplifier output tends to approach the impulse response of the preamplifier. In the high fibre bandwidth region, the situation is similar to that of PCM in that the receiver sensitivity is determined by a balance between erasure and false-alarm errors. It is well known that, under this condition, the optimal filter is a matched filter. However, in PCM a matched filter degrades receiver sensitivity owing to intersymbol interference. In digital PPM, a guard interval is left at the end of each frame, and so this type of interference is not a problem. Hence, in the high fibre bandwidth region the PDD network may be dispensed with, leading to a simplified receiver design.

Referring back to Fig. 8, it can be seen that there is a bandwidth at which the three partial equivocations are equal. This balance in the three error sources suggests that some type of optimum has been achieved. Inspection of Fig. 10, which shows the receiver sensitivity as a func-

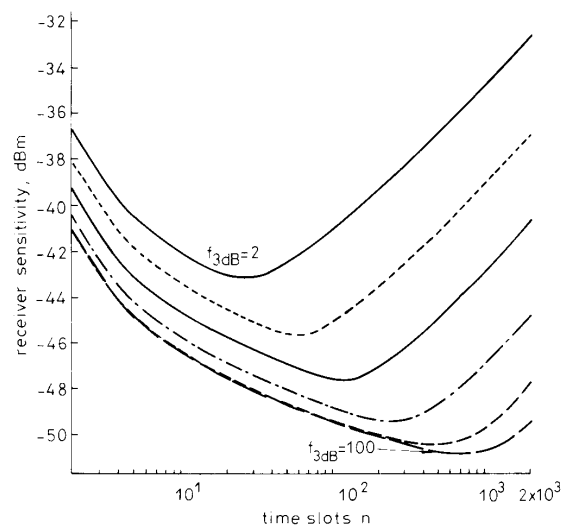


Fig. 10 Receiver sensitivity as a function of n at 50.0 Mbit/s with $m = 0.8$

— normalised fibre bandwidth = 2.0
 - - - normalised fibre bandwidth = 4.0
 — normalised fibre bandwidth = 8.0
 - - - normalised fibre bandwidth = 20.0
 - - - normalised fibre bandwidth = 50.0
 - - - normalised fibre bandwidth = 100.0

tion of the number of time slots n for various receiver bandwidths, reveals that, for a constant fibre bandwidth, there is a value of n that maximises the receiver sensitivity. This optimum does indeed occur when the three partial equivocations are equal. This situation is similar to PCM, in which the optimum sensitivity is achieved when the probability of erasure is the same as the probability of threshold violation. From Fig. 11, it can be seen that increasing the number of time slots above the optimum is comparable to operating in the low-bandwidth region in that wrong-slot errors become predominant. As in the condition of low fibre bandwidth, the pulse energy has to be increased to minimise $H_f(X|Y)$ and $H_r(X|Y)$ and satisfy eqn. 14. Decreasing n below the

optimum results in the peak-to-average power ratio decreasing. This is compensated for by increasing the received pulse energy, which, in turn, leads to the degradation in receiver sensitivity illustrated in Fig. 10. Comparing Fig. 8 and Fig. 11 reveals that the low n region is

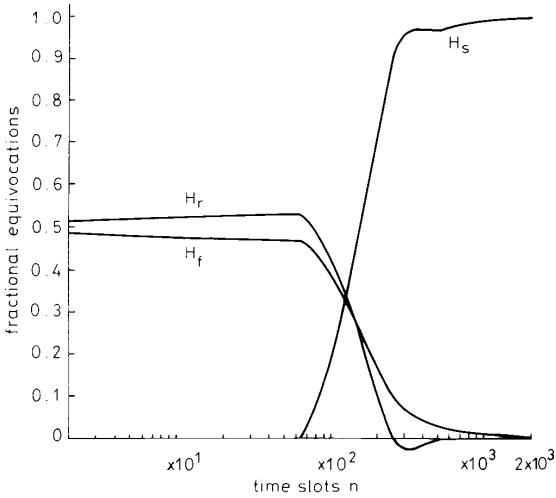


Fig. 11 Fractional equivocation as a function of n at 50 Mbit/s with $m = 0.8$ and $f_{3dB} = 8$

— $H_s(X|Y)$
 - - - $H_r(X|Y)$
 ···· $H_f(X|Y)$

analogous to the high fibre bandwidth region, and so the PDD network may again be dispensed with.

Fig. 12 illustrates the error-rate curves for various fibre bandwidths. To compare the digital PPM system with a

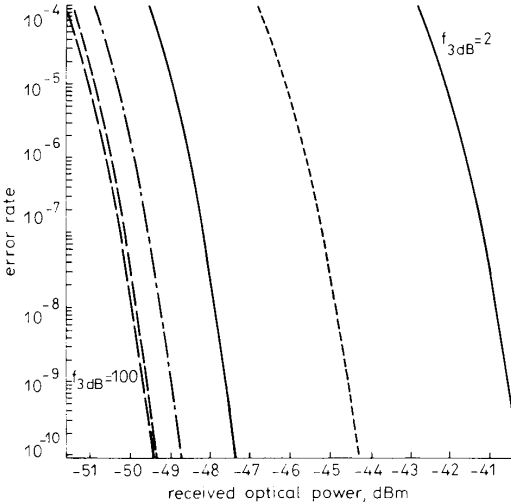


Fig. 12 Receiver error-rate plotted as a function of the received optical power (dBm) at 50.0 Mbit/s with $n = 128$ and $m = 0.8$

— normalised fibre bandwidth = 2.0
 - - - normalised fibre bandwidth = 4.0
 ···· normalised fibre bandwidth = 8.0
 - - - normalised fibre bandwidth = 20.0
 - - - normalised fibre bandwidth = 50.0
 - - - normalised fibre bandwidth = 100.0

commercially available binary PCM system, we consider the optimally biased PIN-BJT preamplifier used in the BT&D advanced function receiver. The measured sensitivity of this type of preamplifier is normally within 1 dB

of that predicted theoretically. The BT&D advanced function receiver is quoted as having a sensitivity of -41.5 dBm ($P_e = 10^{-9}$) when operating at 50 Mbit/s [16]. From Fig. 12, it can be seen that, providing the fibre bandwidth is several times the data rate, the digital PPM system can outperform this commercially available PCM system. For a fibre bandwidth of 1 GHz and a bit error rate of 10^{-9} , the improvement in receiver sensitivity is 7.5 dB.

5 Conclusions

We have analysed the performance of a digital PPM system transmitted over optical fibre channels employing PIN-BJT preamplifiers and assuming a Gaussian received pulse shape. Variational calculus was used to derive an optimal filter for estimating the pulse arrival time, taking into account the three error sources inherent to this form of modulation. The optimal filter was shown to be a matched filter in cascade with a proportional-derivative-delay network. This receiver implementation is simpler than that required for the PIN-FET case, in that a noise whitening filter is not required.

An algorithm has been developed for calculating the receiver sensitivity in terms of the practical system parameters $[v, t_p]$. Digital PPM and binary PCM have been compared on an equivocation-rate basis. Receiver sensitivity calculations predict that digital PPM can usefully out-perform commercially available binary PCM receivers employing optimised PIN-BJT preamplifiers, providing the fibre bandwidth is several times the data rate.

6 Acknowledgments

The authors wish to thank the UK SERC for the CASE award studentship at The Polytechnic, Huddersfield, and BTRL for financing the research contract associated with this project. We also wish to thank the Director of Research and Technology of British Telecommunications PLC, for permission to publish this paper.

7 References

- KARP, S., and GAGLIARDI, R.M.: 'The design of a pulse-position modulated optical communication system', *IEEE Trans.*, 1969, **COM-17**, pp. 61-77
- BORISOV, E.M.: 'Noise immunity of reception of coded messages in optical communication lines', *Radio Eng. Electron. Phys.*, 1978, **24**, pp. 121-124
- KNONOV, A.A., and SHOKIN, Yu.V.: 'Increasing the data transmission speed in optical digital communication channels', *Telecommun. Radio Eng., Part 2*, 1978, **33**, pp. 15-17
- TRUSOV, A.G.: 'Estimation of the optical signal arrival time under conditions of photon counting in free space', *Telecommun. & Radio Eng. Part 2*, 1978, **33**, pp. 137-39
- PIERCE, J.R., POSNER, E.C., and RODEMICH, E.R.: 'The capacity of the photon counting channel', *IEEE Trans.*, 1981, **IT-27**, pp. 61-77
- MECHERIE, G.S.: 'Impact of laser diode performance on data rate capability of PPM optical communication', *Proc. IEEE, MILCOM 85*, 1985, pp. 115-121
- KATZ, J.: 'Average power constraints in AlGaAs semiconductor lasers under PPM conditions', *Opt. Commun.*, 1986, **56**, pp. 330-33
- DAVIDSON, F.M., and SUN, X.: 'Gaussian approximation versus nearly exact performance analysis of optical communication systems with PPM signalling and APD receivers', *IEEE Trans.*, 1988, **COM-36**, pp. 1185-1192
- GARRETT, I.: 'Pulse-position modulation for transmission over optical fibres with direct or heterodyne detection', *ibid.*, 1983, **COM-31**, pp. 518-527
- GARRETT, I.: 'Digital-pulse position modulation over dispersive optical fibre channels'. International Workshop on Digital Communications, Tirrenia, Italy, 15-19 August 1983

- 11 GARRETT, I.: 'Digital pulse-position modulation over slightly dispersive optical fibre channels'. International symposium on Information Theory, St. Jovite, pp. 78-9, 1983
- 12 PIRES, J.J.O., and Da ROCHA, J.R.F.: 'Digital pulse position modulation over optical fibres with avalanche photodiode receivers', *IEE Proc. J.*, 1986, **133**, (5), pp. 309-313
- 13 HELSTROM, C.W.: 'Statistical theory of signal detection' (Pergamon Press, 1968, 2nd edn.), p. 309
- 14 SIBLEY, M.J.N., UNWIN, R.T., and SMITH, D.R.: 'The design of pin-bipolar transimpedance pre-amplifiers for optical receivers', *J. IERE*, 1985, **55**, (3)
- 15 YAMASHITA, K. *et al.*: 'Simple common-collector full-monolithic preamplifier for 560 Mbit/s optical transmission', *Electron. Lett.*, 1986, **22**, pp. 146-147
- 16 SMYTH, P.P.: 'Engineering of optical components for advanced systems' (Laser workshop, University of Essex, 1988)